

A comparison between PMBM Bayesian track initiation and labelled RFS adaptive birth

Ángel F. García-Fernández*, Yuxuan Xia^o, Lennart Svensson^o

*Dept. of Electrical Engineering and Electronics, University of Liverpool, United Kingdom

*ARIES Research Centre, Universidad Antonio de Nebrija, Spain

^oDept. of Electrical Engineering, Chalmers University of Technology, Sweden

Emails: angel.garcia-fernandez@liverpool.ac.uk, firstname.lastname@chalmers.se

Abstract—This paper provides a comparative analysis between the adaptive birth model used in the labelled random finite set literature and the track initiation in the Poisson multi-Bernoulli mixture (PMBM) filter, with point-target models. The PMBM track initiation is obtained via Bayes' rule applied on the predicted PMBM density, and creates one Bernoulli component for each received measurement, representing that this measurement may be clutter or a detection from a new target. Adaptive birth mimics this procedure by creating a Bernoulli component for each measurement using a different rule to determine the probability of existence and a user-defined single-target density. This paper first provides an analysis of the differences that arise in track initiation based on isolated measurements. Then, it shows that adaptive birth underestimates the number of objects present in the surveillance area under common modelling assumptions. Finally, we provide numerical simulations to further illustrate the differences.

Index Terms—Random finite sets, multiple target tracking, adaptive birth, Poisson multi-Bernoulli mixtures, track initiation.

I. INTRODUCTION

Multiple target tracking (MTT) is the process of estimating target trajectories based on noisy sensor data, such as radar and sonar, and has a wide array of applications, including defence, automotive systems and maritime traffic monitoring [1]. Three popular frameworks to solve the multi-target tracking problem are multiple hypothesis tracking [2], joint probabilistic data association [3] and random finite sets (RFS) [4]. These apparently different approaches are closely related to each other, with links established in [5], [6].

In the RFS framework, we require probabilistic models for target birth, dynamics and death, as well as sensor measurements. For the standard point target dynamic and measurement models, and a Poisson point process (PPP) birth model, the posterior density of the set of targets, and also the set of trajectories, is a Poisson multi-Bernoulli mixture (PMBM) [5], [7], [8]. If the birth model is multi-Bernoulli, the posterior density of the set of targets and the set of trajectories is a multi-Bernoulli mixture (MBM) [9], [10]. Both PMBM and MBM filters have hidden/latent variables [11], [12], e.g., representing the underlying data associations and the Bernoulli birth component for multi-Bernoulli birth. For multi-Bernoulli birth, one can make the latent variable that represents time of birth and Bernoulli component explicit in the posterior to

form a labelled RFS. The resulting filter is a labelled MBM filter, whose recursion is analogous to the MBM filter [7]. The MBM filter (labelled or not) can be written with hypotheses with deterministic target existence (MBM₀₁ filter), with an exponential increase in the number of global hypotheses [7]. When labelled, the MBM₀₁ filter corresponds to the widely-used δ -generalised labelled multi-Bernoulli (δ -GLMB) filter [13]. A computationally faster approximation of the δ -GLMB filter is the labelled multi-Bernoulli (LMB) filter [14].

The δ -GLMB and LMB filters work well to estimate target states and trajectories when the multi-Bernoulli birth process allows at maximum one target to be born in a specific location. However, they have difficulties to deal with an independent and identically distributed (IID) cluster birth process covering a large area, in which more than one target may be born at the same time step, for instance, a PPP. In this case, to run the δ -GLMB and LMB filters, we can approximate the PPP as multi-Bernoulli with a sufficient number of components to cover the cardinality distribution, and setting the spatial distribution of the Bernoulli components as in the PPP. The challenge is that these filters would require propagating a large number of global hypotheses to convey the relevant information [15, App. D]. In addition, in this case, the estimated trajectories by the δ -GLMB and LMB filters are not always satisfactory for targets born at the same time step, see Figure 1 and [16, Ex. 2]. This problem could be partially solved by partitioning the surveillance area into a grid, and allowing at maximum one birth with a given label in each cell [17].

Adaptive birth (also called measurement-driven birth) is the most widely-used approach in the labelled RFS literature to deal with large uncertainty in the birth process [14], [18]–[26]. Here, each measurement creates a (labelled) Bernoulli birth component at the following time step. This approach generally works well and mimics track initiation in the PMBM filter, in which each measurement creates a new track, represented as a Bernoulli component. However, in the PMBM filter, the probability of existence and single-target density of a new Bernoulli are obtained via Bayes' rule. In adaptive birth, the single-target density of this Bernoulli component is user-defined and the probability of existence depends on the probability that the measurement is associated to previous targets, also adding a user-defined threshold. While adaptive birth can work well for target and trajectory estimation, the

δ -GLMB filter does no longer provide a recursion to calculate the posterior in closed-form. In particular, target births are dependent on past measurements, which does not agree with assumptions required in the δ -GLMB filter derivation [27].

Adaptive birth has also been adjusted for extended targets [28], merged measurements [29, Fig. 3], simultaneous localisation and mapping [30], and combined with the standard multi-Bernoulli birth [31]. There are also other variations [32] [33]. Another approach to deal with this shortcoming of the δ -GLMB filter is provided in [34]. It should also be mentioned that, in [35], what is referred to as adaptive birth is used in a sequential Monte Carlo probability hypothesis density (PHD) filter implementation. In [35], the birth intensity is actually uniform, and a measurement-driven importance sampling is used for drawing particles [36].

In this paper, we compare the standard adaptive birth method for labelled RFSs with the track initiation in the PMBM filter. To do so, we analyse the differences in track initiation from isolated measurements using both approaches. We also provide an analysis on the expected number of targets for both methods. Finally, we compare both approaches via simulations.

II. MTT MODELS AND TRACK INITIATION

We first provide some background on the standard models for RFS filtering and the filtering recursions in Section II-A. We then review Bernoulli track initiation in PMBM filters in Section II-B. We then review the adaptive birth model for labelled RFSs in Section II-C.

A. Bayesian filtering recursions

In multi-target filtering, we are interested in computing the posterior density of the set X_k of targets at time step k , which is the density of the set of targets given all past and current measurements. At each time step, each target $x \in X_k$ is detected with probability $p^D(x)$ and generates a measurement with conditional density $l(\cdot|x)$. The set Z_k of measurements is the union of the set of target-generated measurements and the set of clutter measurements, which are distributed according to a PPP with intensity $\lambda^C(z)$.

Each target $x \in X_k$ survives to the next time step with probability $p^S(x)$ with a transition density $g(\cdot|x)$. The set X_{k+1} of targets is the union of the set of surviving targets and the set of new born targets at time step $k+1$, which is independent of the set of surviving targets. There are two standard models for target birth: the PPP birth model, with intensity $\lambda_k^B(\cdot)$, and the multi-Bernoulli birth model. With a PPP birth model, the posterior is a PMBM, and with multi-Bernoulli birth model, the posterior is a MBM, which can also be written in MBM₀₁ form [7], [9].

With multi-Bernoulli birth model, one can write the hidden variable $\ell = (k, l)$, where k is the time of birth and l is an index that represents a Bernoulli, explicit in the target state, such that $x = (x', \ell)$, where x' is the dynamic state without label and ℓ is the target label [7, Sec. IV], and define $g(y', \ell_y | x', \ell_x) = g(y' | x') \delta_{\ell_x}[\ell_y]$. In this case, the recursion to compute the posterior is analogous to the MBM case,

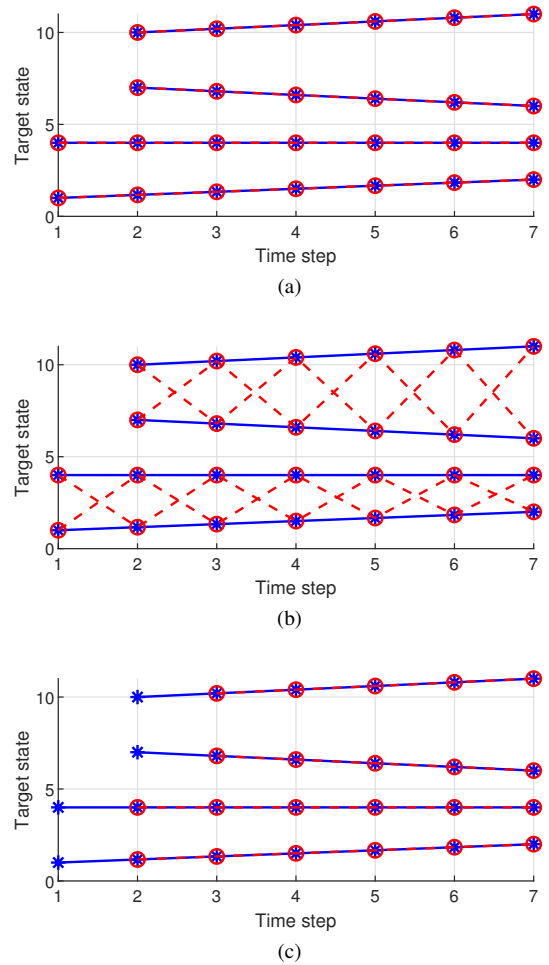


Figure 1: Estimated set of trajectories with $p^D = 1$, $p^S = 1$, accurate measurements, $\bar{\lambda}^C \rightarrow 0$ and an IID cluster birth process that covers the whole surveillance area, allowing more than one target to be born at each time. Blue lines: ground truth set of trajectories. Red dashed line: estimated set of trajectories. Each target cannot move more than 0.5 units at each time step. Subfigure (a): Bayesian solution. Subfigure (b): Track switching for targets born at the same time step. Subfigure (c): Misdetection of targets at the birth time step. Trajectory PMBM and trajectory Poisson multi-Bernoulli (PMB) filters provide (a). The PMBM and PMB filters with sequential track building based on auxiliary variables [15] also provide (a). The filtering densities of the labelled MBM, δ -GLMB and LMB filters do not have information to distinguish between situations (a) and (b), though one can apply the dynamic model to the estimated target states to choose (a). Labelled filters with adaptive birth provide (c) if we select the parameters as $r_{B,max} = 1$, $\bar{\lambda}_2^B \geq 2$ and $\bar{\lambda}_3^B \geq 2$.

but with labelled target states. The MBM₀₁ filter with labels corresponds to the δ -GLMB filter.

B. PMBM Bernoulli track initiation

We proceed to explain how Bernoulli tracks are initialised in PMBM filtering. Given $Z_k = \{z_k^1, \dots, z_k^{m_k}\}$, each measurement generates a new Bernoulli obtained via Bayes' rule. The Bernoulli created by measurement z_k^p has probability of existence and single-target density [5], [7]

$$r_{k|k} = \frac{\langle \lambda_{k|k-1}, p^{Dl}(z_k^p | \cdot) \rangle}{\langle \lambda_{k|k-1}, p^{Dl}(z_k^p | \cdot) \rangle + \lambda^C(z_k^p)} \quad (1)$$

$$p_{k|k}(x) = \frac{p^D(x) l(z_k^p|x) \lambda_{k|k-1}(x)}{\langle \lambda_{k|k-1}, p^D l(z_k^p|\cdot) \rangle} \quad (2)$$

where $\lambda_{k|k-1}(\cdot)$ is the intensity of the PPP representing undetected targets in the PMBM predicted density, and $\langle f, g \rangle = \int f(x) g(x) dx$.

We can then see that the Bayesian approach sets the probability of existence weighting two hypotheses: the probability that the measurement has been generated by a potentially undetected target or clutter. The single-target density takes into account a possibly state-dependent probability of detection, and the state information on undetected targets.

C. Adaptive birth model for labelled RFSs

We proceed to explain how Bernoulli births are set in adaptive birth [14]. Adaptive birth does not use the (labelled) multi-Bernoulli birth mentioned in Section II-A. First, it requires knowledge of the expected number of targets at time step k , which we denote by $\bar{\lambda}_k^B$. Note that $\bar{\lambda}_k^B$ can be obtained from the standard birth models. For PPP birth, we have [4]

$$\bar{\lambda}_k^B = \int \lambda_k^B(x) dx. \quad (3)$$

For multi-Bernoulli birth with n_k^b potential targets, each with a probability of existence r_k^l , we have

$$\bar{\lambda}_k^B = \sum_{l=1}^{n_k^b} r_k^l. \quad (4)$$

Given $Z_k = \{z_k^1, \dots, z_k^{m_k}\}$, the adaptive birth model creates a (labelled) multi-Bernoulli with m_k Bernoulli components at time step $k+1$. The Bernoulli created by $z_k^p \in Z_k$ has a user-defined single-target density $p_{B,k+1}^{(\ell)}(x|z_k^p)$ and probability of existence

$$\hat{r}_{B,k+1}^{(\ell)}(z_k^p) = \min \left(r_{B,max}, \frac{1 - r_{U,k}(z_k^p)}{\sum_{j=1}^{m_k} (1 - r_{U,k}(z_k^j))} \bar{\lambda}_{k+1}^B \right) \quad (5)$$

where $r_{B,max} \in [0, 1]$ is a user-defined parameter that sets a maximum to the existence probability of the new Bernoulli components, and $r_{U,k}(z)$ is the probability that a measurement z is associated to a target in the previous δ -GLMB/LMB hypotheses. In mathematical terms, we have

$$r_{U,k}(z) = \sum_{(I_+, \theta)} 1_\theta(z) w_k^{(I_+, \theta)} \quad (6)$$

where $1_\theta(z)$ is one if $z \in \theta$ and ensures that we sum over updated δ -GLMB/LMB global hypotheses that assign measurement z to one of the targets, $w_k^{(I_+, \theta)}$ is the weight of the updated global hypothesis that contains a set of labels I_+ and data associations θ . Details can be found in [14].

Filtering labelled RFS with adaptive birth model has these properties:

- 1) It can improve the estimated trajectories by δ -GLMB/LMB filters for an IID cluster birth process covering a large area, see Figure 1.

- 2) Target estimation at birth time is delayed at least one time step, see Figure 1.
- 3) The filter no longer has information on undetected targets, which is required, for example, in sensor management [37].
- 4) Target birth depends on past measurements and the δ -GLMB/LMB filter output.
- 5) The δ -GLMB filter is no longer a closed-form recursion to obtain the posterior, as Property 4 does not meet the δ -GLMB filter derivation assumptions, which require that target birth is independent of other targets and measurements.
- 6) Contrary to standard Bayesian filtering modelling [38], there is no generative model of the random variables that represent the states and the measurements that is independent of the filtering algorithm. Therefore, we cannot simulate the ground truth set of targets and measurements by drawing samples from the random process, and, afterwards, carry out filtering.

III. BERNOULLI TRACK INITIATION FROM ISOLATED MEASUREMENTS

In this section, we compare adaptive birth and PMBM Bernoulli track initiation by an isolated measurement that lies in a region where there are no previously detected targets present. We consider this type of scenario as it is easy to analyse and gives insights in the differences. We observe $Z_k = \{z_k^1, \dots, z_k^{m_k}\}$ and consider the assumptions

- A1 Measurement z_k^1 is far away from all potential targets that have been previously detected according to the filter.
- A2 Measurements $z_k^2, \dots, z_k^{m_k}$, $m_k^u \leq m_k$ are far away from z_k^1 and all potential targets that have been previously detected according to the filter.

Sections III-A and III-B explain Bernoulli initiation for PMBM and adaptive birth, respectively. Section III-C illustrates the differences between both methods in three cases.

A. PMBM Bernoulli initiation

Due to A1, the new Bernoulli created by z_k^1 appears in all updated global hypotheses of the PMBM that have non-zero weight. The updated probability of existence and single-target density are given by (1) and (2).

As adaptive birth creates the new Bernoulli components at the following time step, we must perform a prediction on the Bayesian Bernoulli to compare both approaches at the same time step. After the prediction, the probability of existence and single-target density of the Bernoulli are [5]

$$r_{k+1|k} = \langle p_{k|k}, p^S \rangle \quad (7)$$

$$p_{k+1|k}(x) = \frac{\int g(x|y) p^S(y) p_{k|k}(y) dy}{r_{k+1|k}}. \quad (8)$$

The Bayesian approach takes into account $p^D(\cdot)$, $\lambda^C(\cdot)$, $l(z_k^1|\cdot)$ and $\lambda_{k|k-1}(\cdot)$ to obtain (1) and (2), and $p^S(\cdot)$ and $g(\cdot|\cdot)$ to obtain (7) and (8). In addition, the parameters of the Bernoulli are independent of other measurements or previous potential targets.

B. Adaptive birth Bernoulli initiation

Due to A1 and A2, in adaptive birth, the Bernoulli birth components created by measurements $z \in \{z_k^1, \dots, z_k^{m_k^u}\}$ have $r_{U,k}(z) = 0$. The probability of existence of the Bernoulli created by z_k^1 is then

$$\hat{r}_{B,k+1}^{(\ell)}(z_k^1) = \min \left(r_{B,max}, \frac{\bar{\lambda}_{k+1}^B}{m_k^u + \sum_{j=m_k^u+1}^{m_k} (1 - r_{U,k}(z_k^j))} \right), \quad (9)$$

and its single target density $\hat{p}_{k+1|k}(x)$ is user-defined.

Contrary to the Bayesian Bernoulli initiation, the adaptive birth probability of existence (9) depends on the events in other areas through m_k^u and the sum in the denominator. That is, the probability of existence of a Bernoulli created by an isolated measurement is affected by all measurements in the scene. This happens even if they are far-away and do not contain information on this potential target. This can be considered as a type of spooky action at a distance [39].

It should also be noted that, in contrast to the Bayesian approach, adaptive birth does not weight the hypotheses that this measurement has been generated by clutter or by a new detection. In addition, if $m_k = m_k^u$, the probability of existence does not depend on the parameters used in the Bayesian formulation: $p^D(\cdot)$, $\lambda^C(\cdot)$, $l(z_k^1|\cdot)$, $\lambda_{k|k-1}(\cdot)$, $p^S(\cdot)$ and $g(\cdot|\cdot)$.

C. Illustration of differences in three scenarios

We illustrate how both methods behave in three cases in which differences arise. All cases consider $\lambda_{k|k-1}(x) > 0$ and $p^D(x) > 0$.

1) *Case 1:* We consider a scenario without clutter in the area of z_k^1 . For $\lambda^C(z_k^1) = 0$, $p^S(x) = p^S$, the Bayesian approach sets

$$r_{k|k} = 1, \quad r_{k+1|k} = p^S, \quad (10)$$

as this measurement cannot have been originated by clutter. Instead, adaptive birth can set $\hat{r}_{B,k+1}^{(\ell)}$ arbitrarily low if $m_k^u \rightarrow \infty$, which may happen if the clutter intensity or number of targets is high in other areas without previously detected targets.

2) *Case 2:* We consider a scenario in which there is a large number of targets in a far away area with high probability of detection, and $\lambda^C \rightarrow 0$. In this case, we expect a large number m_k^u of received measurements, originated from other targets. The Bayesian solution also sets (10), as it is known that z_k^1 was generated by a new target. In contrast, adaptive birth provides $\hat{r}_{B,k+1}^{(\ell)}(z_k^1) \rightarrow 0$ for $m_k^u \rightarrow \infty$.

3) *Case 3:* We analyse another example with a state-dependent probability of detection and non-uniform clutter. At time step 0, there are no targets with probability one, and we analyse the predicted information at time step 2.

We consider static targets, which could represent landmarks in robotics or mapping [40], [41]. The target state is $x = [x_1, x_2]^T$ where x_1 is position in the x -axis and x_2 is position

in the y -axis. The target birth intensities $\lambda_1^B(\cdot)$ and $\lambda_2^B(\cdot)$ are uniform in the surveillance area $[-l_x, l_x] \times [-l_x, l_x]$, with $l_x = 10$ m.

The probability of detection is 1 in the field of view (FoV), which is a circle of radius $R^D = 5$ m, such that

$$p^D(x) = \begin{cases} 1 & \|x\| \leq R^D \\ 0 & \|x\| > R^D. \end{cases} \quad (11)$$

The single-measurement density for a target-generated measurement $z = [z_1, z_2]^T$ is $l(z|x) = \mathcal{N}(z; x, \alpha I)$, with $\alpha > 0$ being a small number. The clutter intensity is

$$\lambda^C(z) = \begin{cases} 0 & \|z\| \leq R^D \\ \lambda^C & R^D < \|z\|, \|z_1\| < l_x, \|z_2\| < l_x \end{cases} \quad (12)$$

where $\lambda^C > 0$. Therefore, in this scenario, we have almost perfect detections with no clutter in the circle located at the origin with radius R^D . Outside the circle, we cannot detect potential targets and we only have clutter measurements.

Let us consider we observe the measurements in Figure 2(a). The available information in a Bayesian filter, shown in Figure 2(b), is that, at time step 2, the two detections inside the circle are target detections with probability one. Then, there may be undetected targets outside the circle, and we also have target births at time step 2 in the whole surveillance area. On the contrary, the adaptive birth solution in Figure 2(c) does not make use of the knowledge on how p^D and λ^C change spatially, though this information is actually used in the filters to perform prediction and update. The filter incorrectly thinks that there is a potential target with existence probability $\min \left(r_{B,max}, \frac{\bar{\lambda}_2^B}{39} \right)$ created by each of the 39 measurements.

IV. EXPECTED CARDINALITY ANALYSIS

This section analyses the expected number of targets using Bayesian and adaptive birth. To obtain closed-form equations, we analyse the predicted cardinality at time step 2 averaged over all measurements under these conditions

- C1 At time step 0, there are no targets in the surveillance area with probability 1.
- C2 p^S and p^D are constants that do not depend on the target state.

The analysis of the cardinality at time step 1 is not of high interest, as adaptive birth delays target births by one time step, so we consider time step 2. We first provide the Bayesian solution in Section IV-A. Then, we analyse the adaptive birth solution in Section IV-B.

A. Bayesian solution

The MTT system starts at time step 0 with C1, then, targets may be born at time step 1 generating measurements at time step 1 according to the models in Section II-A. At time step 2, new targets may be born. If we average over all possible measurements at time step 1, the predicted number of targets at time step 2 is

$$E[|X_2|] = \iint |X_2| p(X_2, Z_1) \delta X_2 \delta Z_1 \quad (13)$$

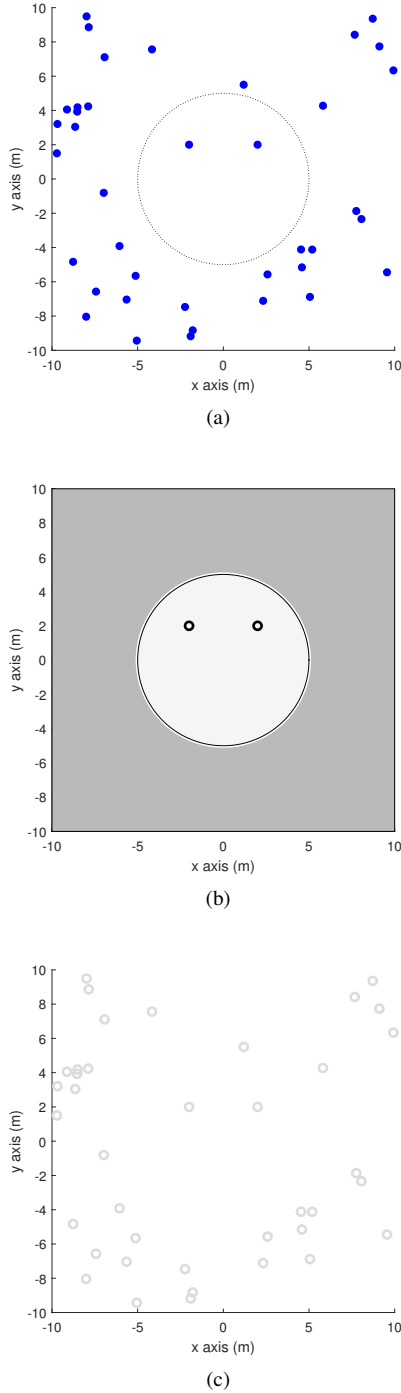


Figure 2: Illustration of Bayesian versus adaptive birth predicted densities $p^S = 1$; $p^D(x) = 1$ and $\lambda^C(z) = 0$ inside the circle, $p^D(x) = 0$ and $\lambda^C(z) > 0$ outside the circle. There are two target generated measurements and 37 clutter measurements. Subfigure (a): measurements at time step 1. Subfigure (b): in the Bayesian solution, there may be unobserved targets outside the FoV, new born targets inside and outside the FoV, and there are also two targets (black circles) inside the FoV with probability one. Subfigure (c): the adaptive birth solution indicates there are 39 potential targets (grey circles), each with a probability of existence $\min\left(r_{B,max}, \frac{\bar{\lambda}_2^B}{39}\right)$, where $r_{B,max}$ is user-defined. In Subfigures (b) and (c), darker areas represent a higher probability of potential targets.

$$= \int |X_2| p(X_2) \delta X_2 \quad (14)$$

$$= p^S \bar{\lambda}_1^B + \bar{\lambda}_2^B \quad (15)$$

where $p(X_2, Z_1)$ is the joint density of X_2 and Z_1 , and $|X|$ denotes the cardinality of set X . That is, the expected number of targets at time step 2 is the expected number of targets born at time step 1 that have survived plus the expected number of targets born at time step 2. Equation (15) can also be obtained by integrating the predicted PHD in the PHD filter [4].

B. Adaptive birth solution

As there are no targets at time step 0, $r_{U,1}(z) = 0$ in (6) for any measurement $z \in Z_1$. This implies that, for $z \in Z_1$, (5) becomes

$$\hat{r}_{B,2}^{(\ell)}(z) = \min\left(r_{B,max}, \frac{\bar{\lambda}_2^B}{|Z_1|}\right). \quad (16)$$

Therefore, for adaptive birth, the predicted number of targets at time step 2 when we receive $|Z_1|$ measurements is

$$\hat{N}(|Z_1|) = \min\left(|Z_1| r_{B,max}, \bar{\lambda}_2^B\right). \quad (17)$$

Then, the expected number of targets averaged over all measurements at time step 2 is

$$\begin{aligned} \hat{E}[|X_2|] &= \int \int |X_2| p(X_2, Z_1) \delta X_2 \delta Z_1 \\ &= \int \hat{N}(|Z_1|) p(Z_1) \delta Z_1 \end{aligned} \quad (18)$$

$$= \sum_{m=0}^{\infty} \min\left(m r_{B,max}, \bar{\lambda}_2^B\right) \rho_{Z_1}(m) \quad (19)$$

$$= r_{B,max} \sum_{m=0}^{\tilde{m}} m \rho_{Z_1}(m) + \bar{\lambda}_2^B \sum_{m=\tilde{m}+1}^{\infty} \rho_{Z_1}(m) \quad (20)$$

$$= \bar{\lambda}_2^B + \sum_{m=0}^{\tilde{m}} \left(r_{B,max} m - \bar{\lambda}_2^B\right) \rho_{Z_1}(m) \quad (21)$$

where $\rho_{Z_1}(m)$ is the probability that set Z_1 contains m elements and

$$\tilde{m} = \left\lfloor \frac{\bar{\lambda}_2^B}{r_{B,max}} \right\rfloor.$$

With adaptive birth model, the distribution $\rho_{Z_1}(\cdot)$ is not specified as there is no generative model for the random variables.

We should note that the expected number of targets of the adaptive birth model meets

$$\sum_{m=0}^{\infty} \min\left(m r_{B,max}, \bar{\lambda}_2^B\right) \rho_{Z_1}(m) \leq \sum_{m=0}^{\infty} \bar{\lambda}_2^B \rho_{Z_1}(m) = \bar{\lambda}_2^B \quad (22)$$

Therefore, the expected number of targets of adaptive birth at time step 2 is always lower or equal than the Bayesian expected number of targets. This result is summarised in the following lemma.

Lemma 1. Under C1 and C2, the predicted number $\hat{E}[|X_2|]$ of targets at time step 2 of adaptive birth is lower or equal than the Bayesian solution $E[|X_2|]$

$$\hat{E}[|X_2|] \leq E[|X_2|]. \quad (23)$$

The inequality is strict if $p^S \bar{\lambda}_1^B > 0$ or there is $m \in \mathbb{N}$ such that $m r_{B,max} < \bar{\lambda}_2^B$ and $\rho_{Z_1}(m) > 0$. In addition, the value of $r_{B,max} \in [0, 1]$ that minimises the cardinality bias gap $E[|X_2|] - \hat{E}[|X_2|]$ is $r_{B,max}^*$.

As the estimated number of targets with adaptive birth is lower than with Bayesian birth under mild conditions, see Lemma 1, we will generally expect that filters with adaptive births miss more targets than filters with Bayesian birth.

V. SIMULATIONS

We compare the performance of Bayesian and adaptive birth via simulations. We have implemented the δ -GLMB and LMB filters¹ with joint prediction and update, using Murty's algorithm [42], with and without adaptive birth. The versions with adaptive birth are referred to as A- δ -GLMB and A-LMB. These filters have been implemented with a maximum number of global hypotheses equal to 1000, and pruning threshold 10^{-10} . LMB has been implemented propagating a single Gaussian, merging threshold 4 and Bernoulli pruning threshold 10^{-3} .

We have implemented the PMBM and PMB filters [5] with Murty's algorithm². We have also implemented adaptive birth, following Section II-C, with the multi-Bernoulli mixture (MBM) filter [7], [9] and multi-Bernoulli (MB) filter. The adaptive MBM (A-MBM) and adaptive MB (A-MB) filters correspond to the PMBM and PMB filters but with the adaptive multi-Bernoulli birth (setting the Poisson intensity equal to zero). This implies that the main difference between A-MBM and PMBM, and A-MB and PMB is the way tracks (Bernoulli components) are initiated. These filters have been implemented with the following parameters [7]: maximum number of global hypotheses $N_h = 200$, threshold for pruning the PPP weights $\Gamma_p = 10^{-5}$, threshold for pruning Bernoulli components $\Gamma_b = 10^{-5}$, estimator 1 with threshold 0.4, and ellipsoidal gating with threshold 20. To speed up running times, all the filters have been implemented with the compiled Murty's algorithm in [43]. All units in this section are in the international system.

A. Models

A target state consists of position and velocity $[p_x, v_x, p_y, v_y]^T$ with a nearly constant velocity model

$$g(x_k | x_{k-1}) = \mathcal{N}(x_k; Fx_{k-1}, Q)$$

$$F = I_2 \otimes \begin{bmatrix} 1 & T \\ 0 & 1 \end{bmatrix}, \quad Q = qI_2 \otimes \begin{bmatrix} T^3/3 & T^2/2 \\ T^2/2 & T \end{bmatrix},$$

where \otimes is the Kronecker product, $q = 0.01$, and the sampling time $T = 1$. We also consider $p_S = 0.995$.

The sensor measures target positions with the model

$$l(z|x) = \mathcal{N}(z; Hx, R)$$

$$H = I_2 \otimes [1 \quad 0], \quad R = I_2.$$

Clutter is uniformly distributed in the region of interest $A = [0, 1000] \times [0, 1000]$ with intensity $\lambda^C(z) = \bar{\lambda}^C \cdot u_A(z)$, where $u_A(z)$ is a uniform density and $\bar{\lambda}^C = 10$. The probability of detection is $p_D = 0.9$.

All filters assume that there are no targets at time 0. Filters with PPP birth have a Gaussian intensity for new born targets with mean $\bar{x}_k^{b,1} = [100, 0, 100, 0]^T$ and covariance matrix $P_k^{b,1} = \text{diag}([150^2, 1, 150^2, 1])$, with weight $w_1^{b,1} = 10$ and $w_k^{b,1} = 0.1$ for $k > 1$. The δ -GLMB and LMB filters use 18 Bernoulli birth components, each with probability of existence $w_1^{b,1}/18$ at time step 1. From time step 2, the birth has one Bernoulli component with probability of existence 0.1. The spatial density of these Bernoulli birth components is the same as for the PPP birth. We use 18 Bernoulli components at time step 1 so that the multi-Bernoulli birth is a reasonable approximation of the PPP birth. The probability of existence is set so that the PPP birth and multi-Bernoulli birth have the same intensity [4]. For adaptive birth, we use (5) with $\bar{\lambda}_k^B = r_{B,max} = w_k^{b,1}$. The user-defined single target-density for adaptive birth is the one in [14]. The mean state is the position indicated by the measurement with zero velocity, and the covariance matrix is $100I_4$.

We draw the ground truth set of trajectories from the generative model with PPP birth and 120 time steps. The resulting sets of trajectories are shown in Figure 3.

B. Simulation results

We assess filter performance via Monte Carlo simulation with 100 runs and obtain the root mean square generalised optimal subpattern assignment (RMS-GOSPA) metric error ($p = 2, c = 10, \alpha = 2$) [44]. The resulting errors as well as the metric decomposition into localisation error for properly detected targets, and costs for missed and false targets are shown in Figure 4. The best performing filters are the PMBM and PMB filters. These are followed by the adaptive birth filters: A- δ -GLMB, A-LMB, A-MBM and A-MB. The δ -GLMB and LMB filters achieve considerably worse performance. The reason for this performance is the high number of hypotheses that are required by δ -GLMB and LMB to keep relevant information, specially when target birth is an IID cluster process covering a large area and more than one target may be born at the same time step [15, App. D]. Adaptive birth filters tend to miss more targets than the PMBM and PMB filters when targets are born.

The computational times to execute one Monte Carlo run of the algorithms on an Intel core i5 laptop are given in Table I. The PMB filter is the fastest algorithm followed by A-MB. These are followed by the PMBM and A-MBM filters. The δ -GLMB and LMB filters are slower due to the MBM₀₁ expansion required in each prediction-update stage and because we consider a higher number of global hypotheses.

¹Matlab code is available at <http://ba-tuong.vo-au.com>.

²Matlab code is available at <https://github.com/Agarciafernandez/MTT>.

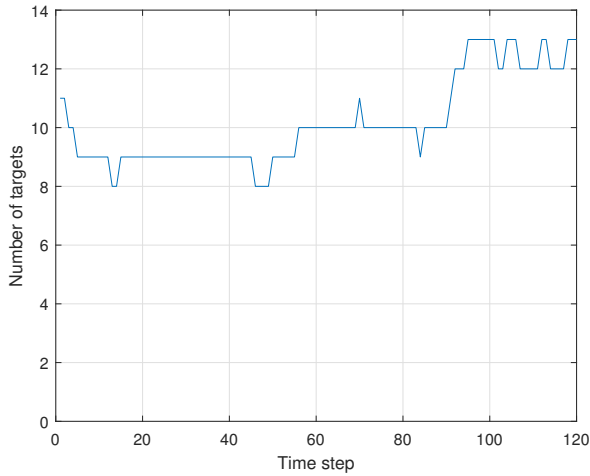
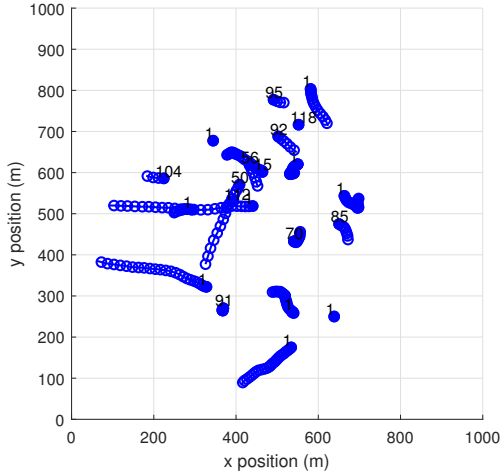


Figure 3: Scenario of the simulations: set of trajectories (top) and number of targets present at each time step (bottom). The number next to each trajectory is its time of birth. The total number of trajectories is 22.

The LMB filter is slower than the δ -GLMB filter in this scenario. In the profile, we can see that the joint prediction and update is faster in LMB, but the function that projects the updated δ -GLMB into an LMB takes considerable time. The δ -GLMB and LMB filters without adaptive birth are faster than with adaptive birth as they consider a maximum of one new born target from time step 2, and therefore fewer hypotheses.

On the whole, we can conclude that filters that do not require an MBM_{01} expansion have important computational benefits. In addition, filters with Bayesian birth are more accurate. Overall PMBM and PMB are the best performing filters in accuracy and computational time.

VI. CONCLUSION

In this paper, we have compared the adaptive birth model used in the labelled RFS framework with the Bernoulli track initiation in PMBM/PMB filters. Adaptive birth resembles the track initiation in PMBM/PMB filters, in which each measurement gives rise to a new Bernoulli. Though not obtained from Bayesian principles, adaptive birth generally works well in scenarios with constant probability of detection and clutter

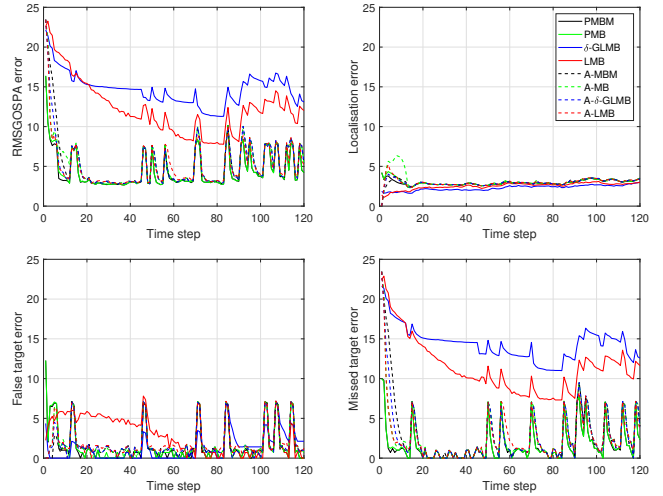


Figure 4: RMS GOSPA errors and their decomposition against time for the considered filters.

intensity. Adaptive birth also improves target and trajectory estimation for the LMB and δ -GLMB filters when the birth model is an IID cluster process with large spatial uncertainty and more than one target may be born at the same time step.

Simulation results show that PMBM/PMB filters outperform filters with adaptive birth to estimate the set of targets, both in accuracy and computational speed. To estimate the set of trajectories, we can use PMBM/PMB with auxiliary variables that can link information from a potential target that was first detected by a given measurement [8], [15], or even better, we can use a PMBM/PMB defined on the set of trajectories of interest [15], [16]. We therefore argue that it is preferable to use fully Bayesian MTT filters based on PPP birth rather than (labelled or unlabelled) multi-Bernoulli adaptive birth.

REFERENCES

- [1] S. Blackman and R. Popoli, *Design and Analysis of Modern Tracking Systems*. Artech House, 1999.
- [2] C.-Y. Chong, S. Mori, and S. Coraluppi, “Forty years of multiple hypothesis tracking,” *Journal of Advances in Information Fusion. Special Issue on Multiple Hypothesis Tracking.*, vol. 14, no. 2, pp. 131–151, Dec. 2019.
- [3] T. Fortmann, Y. Bar-Shalom, and M. Scheffe, “Sonar tracking of multiple targets using joint probabilistic data association,” *IEEE Journal of Oceanic Engineering*, vol. 8, no. 3, pp. 173–184, Jul. 1983.
- [4] R. P. S. Mahler, *Advances in Statistical Multisource-Multitarget Information Fusion*. Artech House, 2014.
- [5] J. L. Williams, “Marginal multi-Bernoulli filters: RFS derivation of MHT, JIPDA and association-based MeMBer,” *IEEE Transactions on Aerospace and Electronic Systems*, vol. 51, no. 3, pp. 1664–1687, July 2015.
- [6] E. Brekke and M. Chitre, “Relationship between finite set statistics and the multiple hypothesis tracker,” *IEEE Transactions on Aerospace and Electronic Systems*, vol. 54, no. 4, pp. 1902–1917, Aug. 2018.
- [7] A. F. García-Fernández, J. L. Williams, K. Granström, and L. Svensson, “Poisson multi-Bernoulli mixture filter: direct derivation and implementation,” *IEEE Transactions on Aerospace and Electronic Systems*, vol. 54, no. 4, pp. 1883–1901, Aug. 2018.
- [8] K. Granström, L. Svensson, Y. Xia, J. L. Williams, and A. F. García-Fernández, “Poisson multi-Bernoulli mixture trackers: continuity through random finite sets of trajectories,” in *21st International Conference on Information Fusion*, 2018, pp. 973–981.

Table I: Computational times in seconds ($\bar{\lambda}^C = 10$)

	PMBM	PMB	δ -GLMB	LMB	A-MBM	A-MB	A- δ -GLMB	A-LMB
Time	3.1	1.9	12.6	23.9	9.7	2.3	49.9	46.8

Table II: RMS-GOSPA errors across time

	PMBM	PMB	δ -GLMB	LMB	A-MBM	A-MB	A- δ -GLMB	A-LMB
$\bar{\lambda}^C = 10$	5.08	5.12	14.82	12.81	6.42	6.15	6.11	5.92
$\bar{\lambda}^C = 20$	5.27	5.30	15.24	12.34	6.82	6.40	6.58	6.26
$\bar{\lambda}^C = 30$	5.51	5.57	12.83	13.95	7.04	6.51	6.86	6.43

- [9] A. F. García-Fernández, Y. Xia, K. Granström, L. Svensson, and J. L. Williams, "Gaussian implementation of the multi-Bernoulli mixture filter," in *Proceedings of the 22nd International Conference on Information Fusion*, 2019.
- [10] Y. Xia, K. Granström, L. Svensson, A. F. García-Fernández, and J. L. Williams, "Multi-scan implementation of the trajectory Poisson multi-Bernoulli mixture filter," *Journal of Advances in Information Fusion*, vol. 14, no. 2, pp. 213–235, Dec. 2019.
- [11] A. P. Dempster, N. M. Laird, and D. B. Rubin, "Maximum likelihood from incomplete data via the EM algorithm," *Journal of the Royal Statistical Society. Series B (Methodological)*, vol. 39, no. 1, pp. pp. 1–38, 1977.
- [12] M. K. Pitt and N. Shephard, "Filtering via simulation: Auxiliary particle filters," *Journal of the American Statistical Association*, vol. 94, no. 446, pp. 590–599, Jun. 1999.
- [13] B.-N. Vo, B.-T. Vo, and D. Phung, "Labeled random finite sets and the Bayes multi-target tracking filter," *IEEE Transactions on Signal Processing*, vol. 62, no. 24, pp. 6554–6567, Dec. 2014.
- [14] S. Reuter, B.-T. Vo, B.-N. Vo, and K. Dietmayer, "The labeled multi-Bernoulli filter," *IEEE Transactions on Signal Processing*, vol. 62, no. 12, pp. 3246–3260, June 2014.
- [15] A. F. García-Fernández, L. Svensson, J. L. Williams, Y. Xia, and K. Granström, "Trajectory Poisson multi-Bernoulli filters," *IEEE Transactions on Signal Processing*, vol. 68, pp. 4933–4945, 2020.
- [16] A. F. García-Fernández, L. Svensson, and M. R. Morelande, "Multiple target tracking based on sets of trajectories," *IEEE Transactions on Aerospace and Electronic Systems*, vol. 56, no. 3, pp. 1685–1707, Jun. 2020.
- [17] A. F. García-Fernández, J. Grajal, and M. R. Morelande, "Two-layer particle filter for multiple target detection and tracking," *IEEE Transactions on Aerospace and Electronic Systems*, vol. 49, no. 3, pp. 1569–1588, July 2013.
- [18] T. T. D. Nguyen, B.-N. Vo, B.-T. Vo, D. Y. Kim, and Y. S. Choi, "Tracking cells and their lineages via labeled random finite sets," *IEEE Transactions on Signal Processing*, vol. 69, pp. 5611–5625, 2021.
- [19] H. V. Nguyen, H. Rezaatofghi, B.-N. Vo, and D. C. Ranasinghe, "Distributed multi-object tracking under limited field of view sensors," *IEEE Transactions on Signal Processing*, vol. 69, pp. 5329–5344, 2021.
- [20] J. Olofsson, C. Veibäck, and G. Hendeby, "Sea ice tracking with a spatially indexed labeled multi-Bernoulli filter," in *20th International Conference on Information Fusion*, July 2017.
- [21] D. Moratuwage, M. Adams, and F. Inostroza, " δ -Generalised labelled multi-Bernoulli simultaneous localisation and mapping," in *International Conference on Control, Automation and Information Sciences*, 2018, pp. 175–182.
- [22] S. Li, W. Yi, R. Hoseinnezhad, G. Battistelli, B. Wang, and L. Kong, "Robust distributed fusion with labeled random finite sets," *IEEE Transactions on Signal Processing*, vol. 66, no. 2, pp. 278–293, 2018.
- [23] S. Li, G. Battistelli, L. Chisci, W. Yi, B. Wang, and L. Kong, "Computationally efficient multi-agent multi-object tracking with labeled random finite sets," *IEEE Transactions on Signal Processing*, vol. 67, no. 1, pp. 260–275, 2019.
- [24] J. Ong, B.-T. Vo, B.-N. Vo, D. Y. Kim, and S. Nordholm, "A Bayesian filter for multi-view 3D multi-object tracking with occlusion handling," *IEEE Transactions on Pattern Analysis and Machine Intelligence*, pp. 1–1, 2020.
- [25] S. Reuter, D. Meissner, B. Wilking, and K. Dietmayer, "Cardinality balanced multi-target multi-Bernoulli filtering using adaptive birth distributions," in *Proceedings of the 16th International Conference on Information Fusion*, 2013, pp. 1608–1615.
- [26] C.-T. Do, T. T. D. Nguyen, D. Moratuwage, C. Shim, and Y. D. Chung, "Multi-object tracking with an adaptive generalized labeled multi-Bernoulli filter," *Signal Processing*, vol. 196, 2022.
- [27] B. T. Vo and B. N. Vo, "Labeled random finite sets and multi-object conjugate priors," *IEEE Transactions on Signal Processing*, vol. 61, no. 13, pp. 3460–3475, July 2013.
- [28] M. Beard, S. Reuter, K. Granström, B.-T. Vo, B.-N. Vo, and A. Scheel, "Multiple extended target tracking with labeled random finite sets," *IEEE Transactions on Signal Processing*, vol. 64, no. 7, pp. 1638–1653, 2016.
- [29] M. Beard, B.-T. Vo, and B.-N. Vo, "Bayesian multi-target tracking with merged measurements using labelled random finite sets," *IEEE Transactions on Signal Processing*, vol. 63, no. 6, pp. 1433–1447, 2015.
- [30] H. Deusch, S. Reuter, and K. Dietmayer, "The labeled multi-Bernoulli SLAM filter," *IEEE Signal Processing Letters*, vol. 22, no. 10, pp. 1561–1565, 2015.
- [31] D. Y. Kim, B.-N. Vo, B.-T. Vo, and M. Jeon, "A labeled random finite set online multi-object tracker for video data," *Pattern Recognition*, vol. 90, pp. 377–389, 2019.
- [32] M. Beard, B. T. Vo, and B. Vo, "A solution for large-scale multi-object tracking," *IEEE Transactions on Signal Processing*, vol. 68, pp. 2754–2769, 2020.
- [33] A. Trezza, D. J. Bucci Jr., and P. K. Varshney, "Multi-sensor joint adaptive birth sampler for labeled random finite set tracking," *IEEE Transactions on Signal Processing*, vol. 70, pp. 1010–1025, 2022.
- [34] K. A. LeGrand and K. J. DeMars, "The data-driven δ -generalized labeled multi-bernoulli tracker for automatic birth initialization," in *Proceedings SPIE Signal Processing, Sensor/Information Fusion, and Target Recognition*, vol. 10646, pp. 1–20.
- [35] B. Ristic, D. Clark, B.-N. Vo, and B.-T. Vo, "Adaptive target birth intensity for PHD and CPHD filters," *IEEE Transactions on Aerospace and Electronic Systems*, vol. 48, no. 2, pp. 1656–1668, April 2012.
- [36] F. Gustafsson, "Particle filter theory and practice with positioning applications," *IEEE Aerospace and Electronic Systems Magazine*, vol. 25, no. 7, pp. 53–82, July 2010.
- [37] P. Boström-Rost, D. Axehill, and G. Hendeby, "Sensor management for search and track using the Poisson multi-Bernoulli mixture filter," *IEEE Transactions on Aerospace and Electronic Systems*, vol. 57, no. 5, pp. 2771–2783, 2021.
- [38] S. Särkkä, *Bayesian Filtering and Smoothing*. Cambridge University Press, 2013.
- [39] D. Franken, M. Schmidt, and M. Ulmke, "'Spooky action at a distance' in the cardinalized probability hypothesis density filter," *IEEE Transactions on Aerospace and Electronic Systems*, vol. 45, no. 4, pp. 1657–1664, Oct. 2009.
- [40] M. Fatemi, K. Granström, L. Svensson, F. J. R. Ruiz, and L. Hammarstrand, "Poisson multi-Bernoulli mapping using Gibbs sampling," *IEEE Transactions on Signal Processing*, vol. 65, no. 11, pp. 2814–2827, 2017.
- [41] H. Durrant-Whyte and T. Bailey, "Simultaneous localization and mapping: part I," *IEEE Robotics Automation Magazine*, vol. 13, no. 2, pp. 99–110, June 2006.
- [42] K. G. Murty, "An algorithm for ranking all the assignments in order of increasing cost," *Operations Research*, vol. 16, no. 3, pp. 682–687, 1968.
- [43] D. F. Crouse, "The tracker component library: free routines for rapid prototyping," *IEEE Aerospace and Electronic Systems Magazine*, vol. 32, no. 5, pp. 18–27, 2017.
- [44] A. S. Rahmathullah, A. F. García-Fernández, and L. Svensson, "Generalized optimal sub-pattern assignment metric," in *20th International Conference on Information Fusion*, 2017, pp. 1–8.